Full Paper

Possible Mechanisms Underlying Statin-Induced Skeletal Muscle Toxicity in L6 Fibroblasts and in Rats

Mai Itagaki[1,2], Akira Takaguri[1], Seiichiro Kano[1], Shigeru Kaneta[1], Kazuo Ichihara[1], and Kumi Satoh[1,*]

[1]*Division of Pharmacology, Hokkaido Pharmaceutical University School of Pharmacy,*
7-1 Katsuraoka, Otaru 047-0264, Japan
[2]*Department of Pharmacy, National Cancer Center Hospital East, 6-5-1 Kashiwanoha, Kashiwa, Chiba 227-8577, Japan*

Abstract. 3-Hydroxy-3-methylglutaryl CoA reductase inhibitors (statins) are safe and well-tolerated therapeutic drugs. However, they occasionally induce myotoxicity such as myopathy and rhabdomyolysis. Here, we investigated the mechanism of statin-induced myotoxicity in L6 fibroblasts and in rats in vivo. L6 fibroblasts were differentiated and then treated with pravastatin, simvastatin, or fluvastatin for 72 h. Hydrophobic simvastatin and fluvastatin decreased cell viability in a dose-dependent manner via apoptosis characterized by typical nuclear fragmentation and condensation and caspase-3 activation. Both hydrophobic statins transferred RhoA localization from the cell membrane to the cytosol. These changes induced by both hydrophobic statins were completely abolished by the co-application of geranylgeranylpyrophosphate (GGPP). Y27632, a Rho-kinase inhibitor, mimicked the hydrophobic statin-induced apoptosis. Hydrophilic pravastatin did not affect the viability of the cells. Fluvastatin was continuously infused (2.08 mg/kg at an infusion rate of 0.5 mL/h) into the right internal jugular vein of the rats in vivo for 72 h. Fluvastatin infusion significantly elevated the plasma CPK level and transferred RhoA localization in the skeletal muscle from the cell membrane to the cytosol. In conclusion, RhoA dysfunction due to loss of lipid modification with GGPP is involved in the mechanisms of statin-induced skeletal muscle toxicity.

Keywords: L6 fibroblasts, statin, skeletal muscle toxicity, cell death, geranylgeranylation

Introduction

3-Hydroxy-3-methylglutaryl-CoA (HMG-CoA) reductase inhibitors (statins) lower the concentrations of low-density lipoprotein cholesterol in blood by blocking the rate-limiting step of the mevalonate pathway. Statins are widely used in patients with hypercholesterolemia (1) to reduce cardiovascular events (2, 3). Although statins are safe and well-tolerated drugs, one of their most important clinical adverse effects in therapy is myo-toxicity, ranging from mild myopathy to serious rhabdo-myolysis. Cerivastatin was voluntarily withdrawn from the market (4) because of the high risk of rhabdomyolysis when used as monotherapy and as co-medication with fibrates. However, the mechanism of statin-induced

myopathy is not yet fully understood. Several hypotheses have been proposed to explain statin-induced myotoxicity, including the lowering of ubiquinone levels (5, 6), alterations of chloride channel conductance within myocytes (7), and apoptosis induction (8 – 10). HMG-CoA reductase, which converts HMG-CoA to mevalonate, is a rate-limiting enzyme of the mevalonate cascade (11). Mevalonate is a precursor not only in cholesterol synthesis but also in the synthesis of iso-prenoid intermediates such as farnesylpyrophosphate (FPP) and geranylgeranylpyrophosphate (GGPP). These intermediates are important for post-translational iso-prenylation of a number of proteins including small G proteins such as Ras, Rho, and Rab (12). Therefore, blockade of the mevalonate pathway by statins can affect critical cellular functions. We previously reported that atorvastatin impairs glucose uptake in 3T3L1 adipocytes associated with attenuation of the localization of RhoA to the cell membrane (13). A deficit in compounds bio-

synthesized in the mevalonate pathway may adversely affect skeletal muscle. In the present study, we investigated the effects of statins on L6 fibroblasts derived from the rat skeletal muscle in vitro and rat skeletal muscles in vivo.

Materials and Methods

Drugs and reagents

Pravastatin, simvastatin, and fluvastatin were kindly provided by Daiichi-Sankyo Co. (Tokyo). Y27632 was purchased from Calbiochem (San Diego, CA, USA). Anti-RhoA antibody was obtained from Santa Cruz Biotechnology (Santa Cruz, CA, USA). Anti-mouse immunoglobulin G secondary antibody was purchased from Cell Signaling Technology (Bevery, MA, USA). Aporotinin, phenylmethylsulfonylfluoride (PMSF), leupeptin, bovine serum albumin, *dl*-mevalonic acid lactone, FPP ammonium salt, and GGPP ammonium salt were bought from Sigma (St. Louis, MO, USA). Dulbecco's modified Eagle's medium-low glucose containing 1 g/mL glucose (DMEM-low glucose) and CPK-II test Wako were purchased from Wako Pure Chemical Industries, Ltd. (Osaka). Fetal bovine serum (FBS) was obtained from Invitrogen (Carlbad, CA, USA). WST-8,4',6-diamidino-2-phenylinodole (DAPI), and a cell counting kit were purchased from Dojindo Laboratories (Kumamoto). COD-Star Reagent was obtained from New England BioLabs (Ipswich, MA, USA).

Cell culture

L6 fibroblasts were obtained from the Health Science Research Resources Bank (Osaka) and grown in DMEM-low glucose–containing 10% FBS at 37°C in humidified atmosphere of 5% CO_2 until approx. 80% confluence. To induce differentiation, cells were further cultured in medium containing 1% FBS.

Cell viability

Cell viability was assessed by measuring the activity of mitochondrial dehydrogenase using the tetrazolium compound WST-8 (14). L6 fibroblasts (5×10^3 cells /mL) were seeded into a 96-well plate and incubated for 24 h. Following treatment with statins at certain concentrations for the periods indicated, WST-8 was added and incubated for 2 h. Cellular activities were determined by measuring absorbance at 450 nm using a microtiter-plate reader.

DAPI staining

To detect morphological evidence of apoptosis, cell nuclei were visualized following DNA staining with the fluorescent dye DAPI (15). After incubation for 24 h in DMEM-low glucose–containing 10% FBS, cells were treated with 50 μM fluvastatin or simvastatin in DMEM-low glucose–containing 1% FBS for 48 h. Then, cells were washed three times with phosphate-buffered saline (PBS), fixed with 3% paraformaldehyde for 10 min, and then labeled with DAPI (1 μg/mL) for 10 min. After labeling, apoptotic cells were visualized under a fluorescence microscope (Olympus, Melville, NY, USA).

Caspase-3 activity

After incubation of L6 fibroblasts for 12 h with 50 μM statin in the presence or absence of GGPP or FPP, caspase-3 activity was assayed using BD ApoAlert™ Caspase Assay plates (Biosciences Clontech, Mountain View, CA, USA). Briefly, following incubation of cells (2×10^5) with 50 μM fluvastatin, simvastatin, or Y27632, cells were lysed in lysis buffer (25 mM Tris (pH 7.5), 150 mM NaCl, 10 mM sodium fluoride, 1 mM sodium vanadate, 1 mM PMSF, 10 μg/ml aprotinin, 10 μg/ml leupeptin, and 1% Nonidet 40) for 10 min on ice. After centrifugation, 50 μL of cell lysates and 50 μL of reaction buffer/dithiothreitol mixture were incubated at 37°C for 2 h. Caspase-3 activities were determined by a fluorescent plate reader with the excitation wavelength at 380 nm and emission at 465 nm.

Subcellular fraction and immunoblotting

Cell cytosolic and membrane fractions were prepared as described previously (16). The cell homogenate was centrifuged at $100,000 \times g$ for 20 min at 4°C to separate the cytosolic and crude membrane fractions. Membranes were suspended in Nonidet P-40 lysis buffer (25 mM Tris-HCl (pH 7.5), 1% Nonidet P-40, 150 mM NaCl, 10 mM NaF, 1 mM Na_3VO_4, 1 mM PMSF, and 10 μg/ml each of leupeptin and aprotinin). Insoluble materials were removed by centrifugation at $20,000 \times g$ for 5 min at 4°C, and the resulting supernatant was referred to as the solubilized membrane fraction. All procedures were performed at 4°C. For immunoblotting, cell lysates or the subcellular fraction was subjected to sodium dodecyl sulfate polyacrylamide gel electrophoresis and transferred to polyvinylidene difluoride membranes. Samples were probed with anti-RhoA antibody and detected using the COD-Star Reagent with alkaline phosphatase–conjugated secondary antibodies, according to the manufacturer's protocol.

Animal preparation

The present investigation conforms to the Guiding Principles for the Care and Use of Experimental Animal of Hokkaido Pharmaceutical University (published 1998, revised 2001 and 2007). Male Wister rats (4 – 5

weeks of age) were obtained from Sankyo Labo Service Corporation (Machida, Tokyo). Animals were housed under controlled temperature (23°C) and lighting (12-h light / 12-h dark cycle) with free access to water and standard rat chow. After 1 week of feeding with a chow diet, rats were randomly assigned to the control group (n = 5) or fluvastatin-treated group (n = 5). Rats were anesthetized with pentobarbital (30 mg/kg, i.p.) and an indwelling catheter was inserted into the right internal jugular vein for drug infusion. The catheter was inserted subcutaneously to exit dorsally at the midscapular region and was covered with a stainless steel extension spring. The spring was secured to the rat by a rigid polyethylene neck (90° angle) sutured subcutaneously at the exit incision. The spring and catheter were then suspended from a contort holder directly above the cage, ensuring the rat 360° of free and unrestricted motion. Heparinized saline (10 IU/mL) was infused into the catheter to prevent blood coagulation. Two days after cannulation, fluvastatin [2.08 mg/kg at an infusion rate of 0.5 mL/h (or 50 mg/kg per day)] was infused continuously into the rats through a jugular catheter for 72 h.

Measurement of plasma fluvastatin concentration

After 72 h of infusion, plasma fluvastatin concentration was determined using a high-performance liquid chromatography (HPLC) system equipped with a UV detector (17). The column used was a WAKOPAK Handy ODS (4.6 mmø × 250 nm), and the mobile phase consisted of an aqueous solution containing 20 mM dibasic sodium dihydrogen phosphate with 1 mM sodium lauryl sulfate adjusted to pH 7 with phosphoric acid and acetonitrile (70:30 v/v). The column temperature and flow rate were 50°C and 1.0 mL/min, respectively.

Tissue fractionation and immunoblotting

Seventy-two hours after fluvastatin infusion, skeletal muscles were immediately removed and frozen in liquid nitrogen. Tissue samples were stored at −80°C for later analysis. Tissues were homogenized using a Teflon homogenizer in Tris-buffer and centrifuged at $600 \times g$ for 10 min at 4°C. The cytosolic and crude membrane fractions were prepared as described in the "*Subcellular fraction and immunoblotting*" section. The samples were immunoblotted with anti-RhoA antibody, as described above.

Measurement of plasma CPK levels

Before and at 48 and 72 h after starting the fluvastatin infusion, blood samples were taken via the jugular catheter for measurement of plasma CPK levels using CPK-II test Wako.

Statistical analyses

Each value was expressed as the mean ± S.E.M. Significance of the differences between groups was evaluated by one-way analysis of variance followed by Dunnett's *t*-test with Stat View (SAS Institute Inc., Cary, NC, USA). Statistical significance was defined as *P*<0.05.

Results

Cell viability

Treatment with the hydrophobic statins simvastatin and fluvastatin significantly decreased the viability of L6 fibroblasts in a dose-dependent manner (Fig. 1). Pravastatin, a hydrophilic statin, showed no effect on cell viability at the doses tested. The concentrations decreasing cell viability to 50% were $2.1 \pm 0.1 \mu M$ for simvastatin and $1.6 \pm 0.1 \mu M$ for fluvastatin.

Effects of statins on DAPI staining and activity of caspase-3

Fragmented nuclei were observed in L6 fibroblasts treated with simvastatin and fluvastatin at $10 \mu M$ for 48 h (Fig. 2A). Treatments with simvastatin and fluvastatin at $10 \mu M$ for 16 h significantly increased caspase-3 activity in L6 fibroblasts compared with the control cells (Fig. 2B).

Co-application of GGPP or FPP with statin

Simvastatin and fluvastatin at $50 \mu M$ decreased cell viabilities to $25 \pm 6\%$ and $36 \pm 9\%$ relative to those of the control cells, respectively. The decreased cell viabilities induced by simvastatin and fluvastatin were
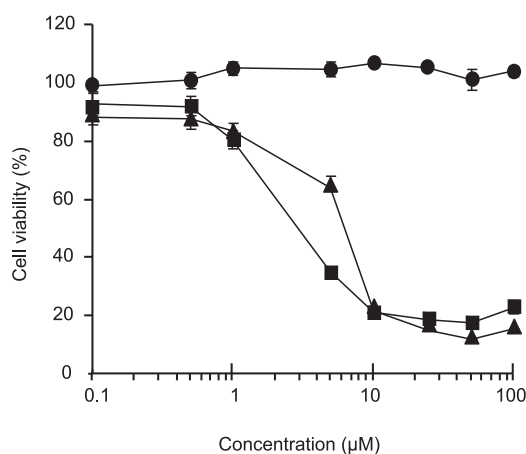

Fig. 1. Effects of statins on viability of L6 fibroblasts. L6 fibroblasts were treated with $0.1 – 100 \mu M$ simvastatin (solid square), fluvastatin (solid triangle), or pravastatin (solid circle) for 48 h and then incubated with WST-8 for another 2 h. Activity of mitochondrial dehydrogenase was determined by measuring absorbance at 450 nm using a microtiter-plate reader. Each point represents a mean ± S.E.M. (n = 4).
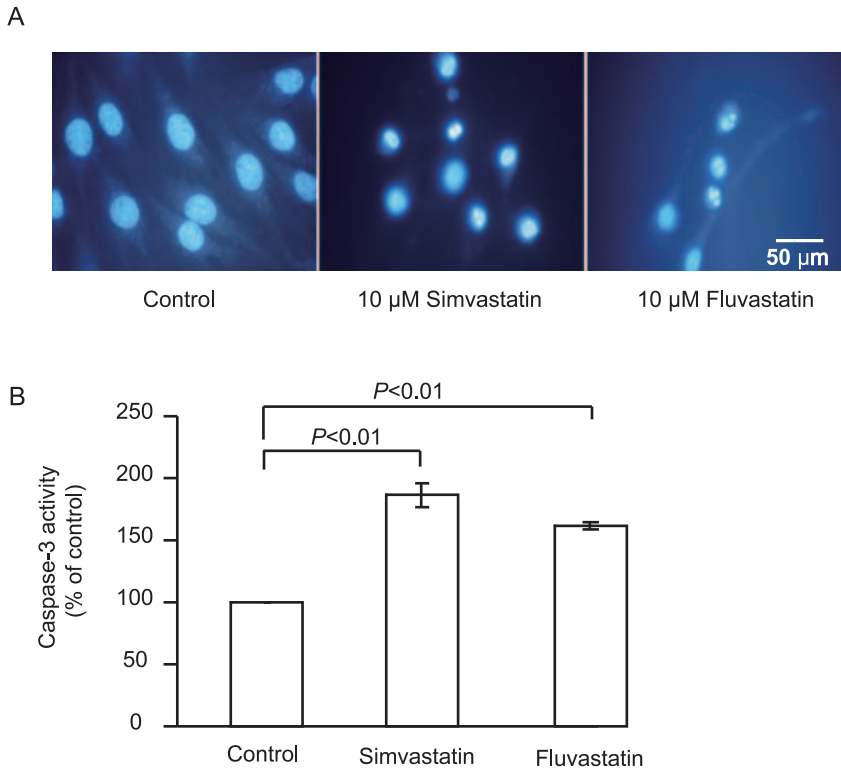
A

B

Fig. 2. DAPI staining and caspase-3 activity of L6 fibroblasts treated with fluvastatin or simvastatin. A: Forty-eight hours after treatment with $10\,\mu$M fluvastatin or simvastatin, L6 fibroblasts were fixed and stained with the nuclear dye DAPI. Nuclear morphology was visualized by fluorescent microscopy. B: L6 fibroblasts were treated with $10\,\mu$M fluvastatin and simvastatin for 16 h and caspase-3 activity was determined using BD ApoAlert™. Each column represents a mean $\pm$ S.E.M. (n = 4).

completely recovered by the co-application of GGPP; however, that of FPP induced only low recovery (Fig. 3A). Also, simvastatin and fluvastatin increased caspase-3 activity. The effect of simvastatin on caspase-3 activity was more potent than that of fluvastatin. Similarly, the co-application of GGPP decreased caspase-3 activity, which had been increased by simvastatin and fluvastatin to the level of the control cells (Fig. 3B). The co-application of FPP did not reverse the effects of simvastatin and fluvastatin on cell viability and caspase-3 activity.

Subcellular distribution of RhoA in L6 fibroblasts

Figure 4 shows the localization of RhoA in the cell membrane and cytosolic fractions. RhoA, a small G-protein, requires lipid modification with GGPP for its localization to the cell membrane and for retaining its biological functions. RhoA in the control cells was localized more in the cell membrane than in the cytosol. Treatment with simvastatin or fluvastatin prevented RhoA translocation to the cell membrane, increasing cytosolic RhoA. The co-application of mavalonate and GGPP but not FPP restored the subcellular distribution of RhoA that was changed by simvastatin and fluvastatin (Fig. 4).

Effects of Y27632 on L6 cell viability and caspase-3 activity

Y27632 is a selective inhibitor of Rho-associated protein kinase. The effects of Y27632 on the cell viability and activity of caspase-3 in L6 fibroblasts are shown in Fig. 5. Treatment of L6 fibroblasts with Y27632 at $>10\,\mu$M for 48 h significantly reduced cell viability in a dose-dependent manner (Fig. 5A), and that at $50\,\mu$M for 16 h significantly increased caspase-3 activity (Fig. 5B). Y27632 caused cell death and activation of casepase-3 in the L6 fibroblasts similar to those caused by the hydrophobic statins.

Effect of wortmannin on cell viability

The effect of wortmannin on the viability of L6 fibroblasts is shown Fig. 6. L6 fibroblasts were treated with wortmannin at $1-500$ nM for 48 h. Because wortmannin showed no affect on cell viability even at 500 nM, statin-induced apoptosis of L6 fibroblasts might be independent of the PI3-Ras pathway.

Fluvastatin infusion into rats in vivo

Figure 7 shows the plasma concentration of fluvastatin (A) and plasma CPK levels (B) in blood obtained from rats before and at 48 and 72 h after intravenous infusion of fluvastatin or saline as control. The plasma concentration of fluvastatin at 72 h after starting infusion
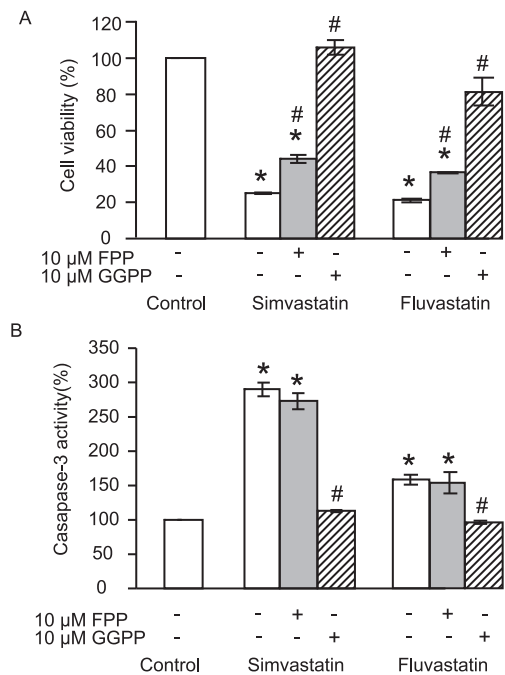
Fig. 3. Effects of co-application of GGPP or FPP with statin on cell viability and caspase-3 activity A: L6 fibroblasts were treated for 48 h with 50 μM fluvastatin or simvastatin in the absence or presence of 10 μM FPP or GGPP. The cells were incubated with WST-8 for an additional 2 h. Activity of mitochondrial dehydrogenase was determined by measuring absorbance at 450 nm using a microtiter-plate reader. B: L6 fibroblasts were treated with 50 μM fluvastatin or simvastatin for 16 h in the absence or presence of 10 μM FPP or GGPP. Caspase-3 activity of was determined using BD ApoAlert™. Each column represents a mean ± S.E.M. (n = 4). *P<0.05 vs control, #P<0.05 vs statin alone.
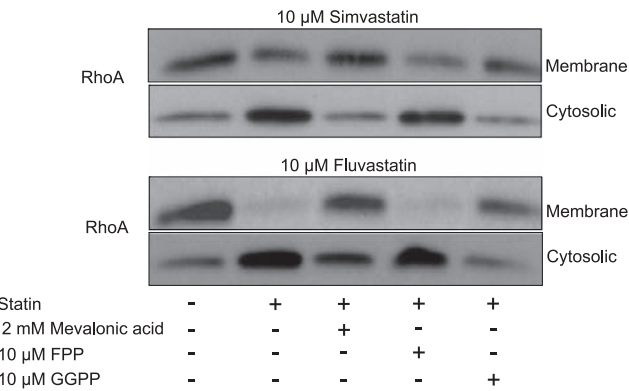

Fig. 4. Effects of statins on subcellular distribution of RhoA. L6 fibroblasts were treated with 10 μM fluvastatin or simvastatin for 48 h in the presence or absence of 2 mM mevalonic acid, 10 μM FPP, or GGPP. The cells were fractionated into the crude membrane and cytosol, and the amount of RhoA was determined by immunoblotting analysis using anti-RhoA antibody.
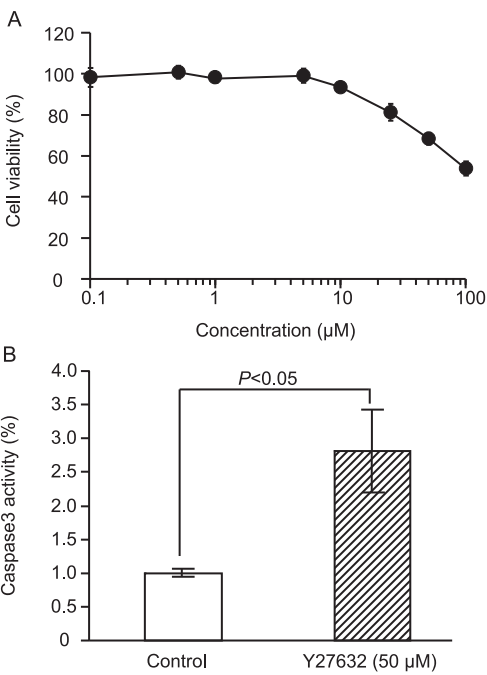

Fig. 5. Effects of Y27632 on viability and caspase-3 activity of L6 fibroblasts. A: L6 fibroblasts were treated for 48 h with various concentrations of Y27632, and cell viability was determined by the WST-8 method. Each point represents a mean ± S.E.M. (n = 4). B: L6 fibroblasts were treated with 50 μM Y27632 for 16 h. Caspase-3 activity was determined using BD ApoAlert™. Each column represents a mean ± S.E.M. (n = 3).
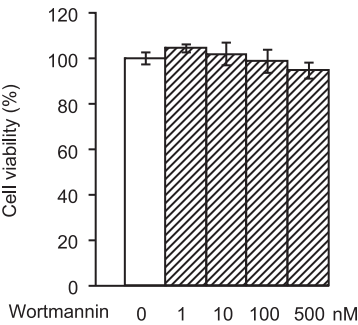

Fig. 6. Effect of wortmannin on viability of L6 cells. L6 fibroblasts were treated with various concentrations of Y27632 for 48 h, and cell viability was determined by the WST-8 method.

plasma CPK levels in the fluvastatin-infused rats were significantly higher than those in the saline-infused control rats.

Subcellular distribution of skeletal muscle RhoA in rats

The subcellular distribution of RhoA in the skeletal muscle of rats is shown in Fig. 8. RhoA in the skeletal muscle of the saline-infused control rats was localized considerably more in the cell membrane than in the
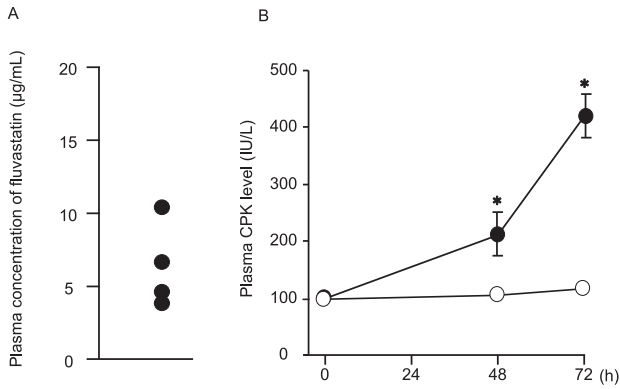
was 6.02 ± 1.19 μg/mL. This concentration is equivalent to 13.9 μM and approximately the same concentration as that of the statin applied to L6 fibroblasts in vitro. The

Fig. 7. Plasma concentration of fluvastatin and serum CPK level in rats. A: Fluvastatin (50 mg/kg per day, 0.5 mL/h) was intravenously infused into rats for 72 h. At 72 h after starting the infusion of fluvastatin, its plasma concentration was determined using an HPLC system equipped with a UV detector. Each point represents the plasma concentration of each rat (n = 5). B: Before and at 48 and 72 h after starting fluvastatin infusion, serum CPK levels were determined using CPK-II test Wako. Each column represents a mean ± S.E.M. (n = 5). *$P < 0.05$ vs control.
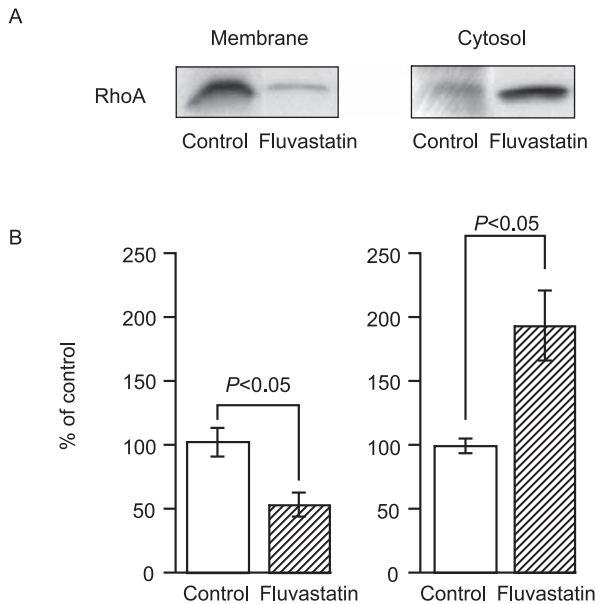

Fig. 8. Effects of statins on subcellular distribution of RhoA in rat skeletal muscle. Fluvastatin or saline (50 mg/kg per day, 0.5 mL/h) was intravenously infused for 72 h into rats. At 72 h after fluvastatin or saline infusion, skeletal muscles were immediately removed and fractionated into the cell membrane and cytosol fractions. Amounts of RhoA protein are expressed as the percentage of that in the untreated (control) cells (mean ± S.E.M of 5 independent observations).

cytosol. Fluvastatin clearly decreased the amount of RhoA distributed in the cell membrane. This in vivo result is in agreement with the result obtained in L6 cells in vitro.

Discussion

The present study demonstrated that simvastatin and fluvastatin concentration-dependently decreased cell viability, while pravastatin showed no effect even at 100 μM (Fig. 1). This result is in agreement with that previously reported for rat pulmonary vein endothelial cells (18). It has been shown that membrane permeabilities among HMG-CoA reductase inhibitors are different (19). Simvastatin and fluvastatin are hydrophobic compounds that cannot easily enter any cell and they inhibit HMG-CoA reductase (20). In contrast, pravastatin is a hydrophilic compound that cannot penetrate the cell membrane; however, it can inhibit HMG-CoA reductase in hepatic cells because the hepatic cell membrane contains organic anion transporters that transport hydrophilic substances into cells (21). Simvastatin, fluvastatin, and pravastatin are therefore equally effective in lowering cholesterol concentration in blood. Since pravastatin showed no effect on cell viability, we investigated the mechanism of cell death induced by hydrophobic statins.

In DAPI nuclear staining, fragmented nuclei were observed in L6 cells treated with fluvastatin or simvastatin at 10 μM for 48 h (Fig. 2A). DAPI is a blue nucleic acid fluorescence dyeing agent and attaches to the DNA strand spiral gutter. When a cell dies, chromosome agglutination and DNA fragmentation occur (14). In addition, fluvastatin and simvastatin significantly elevated caspase-3 activity in L6 fibroblasts (Fig. 2B). First, cells were treated with simvastatin or fluvastatin at 10 μM (Fig. 2) to examine whether statin-induced cell death was due to apoptosis. Since the results revealed that both statins induced apoptosis, we used them in higher concentrations to observe a dose-dependent increase in caspase-3 activity (Fig. 3). Activation of caspase-3 was concentration-dependent for simvastatin treatment, but fluvastatin-induced activation peaked at 10 μM. These results suggest that the statin-induced cell death could be due to apoptosis. Apoptosis in skeletal muscle cells may trigger different forms of myotoxicity such as myopathy and rhabdomyolysis.

HMG-CoA reductase, which converts HMG-CoA to mevalonate, is a rate-limiting enzyme of the mevalonate cascade (11). Mevalonic acid is a precursor not only in cholesterol synthesis but also in the synthesis of isoprenoid intermediates such as FPP and GGPP. Geranylgeranylation and farnesylation are required by small G proteins such as Ras and Rho, which play crucial roles in cell growth and differentiation. The co-application with GGPP prevented statin-induced cell death, while that with FPP did not (Fig. 3). In the present study, exposure of L6 fibroblasts to simvastatin and

fluvastatin decreased the amount of RhoA in the membrane fraction, but increased its amount in the cytosolic fraction (Fig. 4). Y27632, a selective inhibitor of Rho-associated protein kinase, mimicked the effects of hydrophobic statins on cell viability and caspase-3 activity (Fig. 5). These results further indicate that dysfunction of RhoA is associated with statin-induced apoptosis.

However, several investigators have reported depletion of other membrane-bound small G proteins in statin-induced myotoxicity. Matzno et al. (8) reported that statin-induced apoptosis in L6 fibroblasts was related to Ras depletion in the membrane, but not RhoA depletion. In the present study, Ras dysfunction was not responsible for statin-induced cell death in fibroblasts because pretreatment with FPP did not completely prevent it, and wortmannin did not mimic the effect of statin on cell viability (Fig. 6). Since Matzno et al. observed the early phase of apoptosis (0 – 6 h after cerivastatin treatment) in contrast to our experiments, depletion of different small G proteins during the progression of apoptosis might be involved in the statin-induced apoptosis pathway. Alternatively, Sakamoto et al. (22) reported that Rab is involved in fluvastatin-induced formation of vacuoles in myofibers (although we did not examine Rab involvement).

Simvastatin seems to have greater effects on cell viability and caspase-3 activity than fluvastatin; however, pravastatin showed no effects on L6 fibroblasts. Moreover, the lipophilicity of simvastatin is higher than that of fluvastatin, and that of pravastatin is less than that of fluvastatin. Statins with high lipophilicity easily penetrate into cells and inhibit HMG-CoA reductase. Therefore, the degree of lipophilicity of statins may be correlated with their sensitivity to cells. This may also apply to clinical practice because cerivastatin, which has the highest lipophilicity among statins, has been voluntarily withdrawn from the market due to high risk of rhabdomyolysis (10). In the present study, pravastatin showed no effect even at the highest concentration of 100 μM. However, it had an effect on L6 fibroblasts at a much higher concentration (3 mM) (8) and carries the risk of myopathy in clinical practice, although the incidence is less than the other statins.

Sakamoto et al. (22) have reported that there is a difference in the effects of statins on signal transduction between immortalized skeletal muscle cell lines such as L6 fibroblasts and freshly isolated myofibers. Therefore, we conducted an in vivo study in line with the above-mentioned work by infusing fluvastatin into rats. Although statins have been orally administered in clinical practice, fluvastatin (2.08 mg/kg at an infusion rate of 0.5 mL/h) in the present study was infused continuously into rats via a jugular vein catheter for 72 h. In several in vivo studies, the severity of muscle injury induced by oral treatment of statin varied greatly between individual animals. The model used in the present study allows the maintenance of a constant blood concentration of fluvastatin, which can rapidly and conveniently induce myotoxicity. Since simvastatin does not practically dissolve in saline owing to its high lipophilicity (octanol-water partition coefficient: simvastatin, 25,118; fluvastatin, 55), we employed fluvastatin in the in vivo study. Before and at 48 h and 72 h after starting fluvastatin infusion, blood samples were taken and plasma CPK level was measured. CPK levels in fluvastatin-infused rats 48 and 72 h after starting the infusion were higher than those in the control rats (Fig. 7). Elevation of plasma CPK is one of the clinical signs of rhabdomyolysis (23). The plasma concentration of fluvastatin 72 h after starting the infusion was 6.02 ± 1.19 μg/mL, which is equivalent to 13.9 μM and is approximately the same concentration as the applied statin dose in L6 fibroblasts. The amounts of RhoA in the cell membrane fraction of skeletal muscles in fluvastatin-infused rats were significantly lower than those of the saline-infused rats (Fig. 8), which is in accordance with the result obtained in L6 fibroblasts (Fig. 4).

In conclusion, the results suggest that fluvastatin induces apoptosis in L6 fibroblasts and myopathy in rat skeletal muscles through RhoA inactivation resulting from GGPP attenuation. However, the mechanism of RhoA-induced myopathy in vivo remains to be investigated.

References

1 Shepherd J, Cobbe SM, Ford I, Isles CG, Lorimer AR, Macfarlane PW, et al. Prevention of coronary heart disease with pravastatin in men with hypercholesterolemia. N Engl J Med. 1995;333:1301–1307.

2 Schwartz GG, Olsson AG, Ezekowitz MD, Ganz P, Oliver MF, Waters D, et al. Effects of atorvastatin on early recurrent ischemic events in acute coronary syndromes: the MIRACL study: a randomized controlled trial. JAMA. 2001;285:1711–1718.

3 Illingworth DR, Tobert JA. A review of clinical trials comparing HMG-CoA reductase inhibitors. Clin Ther. 1994;16:366–385.

4 FDA talk paper. Bayer voluntarily withdraws Baycol on August 2001.

5 Yamazaki H, Suzuki M, Aoki T, Morikawa S, Maejima T, Sato F, et al. Influence of 3-hydroxy-3-methylglutaryl coenzyme A reductase inhibitors on ubiquinone levels in rat skeletal muscle and heart: relationship to cytotoxicity and inhibitory activity for cholesterol synthesis in human skeletal muscle cells. J Atheroscler Thromb. 2006;13:295–307.

6 Marcoff L, Thompson PD. The role of coenzyme Q10 in statin-

associated myopathy: a systematic review. J Am Coll Cardiol. 2007;49:2231–2237.

7 Pierno S, Didonna MP, Cippone V, De Luca A, Pisoni M, Frigeri A, et al. Effects of chronic treatment with statins and fenofibrate on rat skeletal muscle: a biochemical, histological and electrophysiological study. Br J Pharmacol. 2006;149:909–919.

8 Matzno S, Yasuda S, Juman S, Yamamoto Y, Nagareya-Ishida N, Tazuya-Murayama K, et al. Statin-induced apoptosis linked with membrane farnesylated Ras small G protein depletion, rather than geranylated Rho protein. J Pharm Pharmacol. 2005;57:1475–1484.

9 Driks AJ, Jones KM. Statin-induced apoptosis and skeletal myopathy. Am J Physiol Cell Physiol. 2006;291:C1208–C1212.

10 Lamperti C, Naini AB, Lucchini V, Prelle A, Bresolin N, Moggio M, et al. Muscle coenzyme Q10 level in statin-related myopathy. Arch Neurol. 2005;62:1709–1712.

11 Goldstein L, Brown S. Regulation of the mevalonate pathway. Nature. 1990;343:425–430.

12 Hughes D. The role of isoprenoids in vascular smooth muscle: potential benefits of statins unrelated to cholesterol lowering. J Hum Hypertens. 1996;10:387–390.

13 Takaguri A, Satoh K, Itagaki M, Tokumitsu Y, Ichihara K. Effects of atorvastatin and pravastatin on signal transduction related to glucose uptake in 3T3L1 adipocytes. J Pharmacol Sci. 2008;107:80–89.

14 Ishiyama M, Tominaga H, Shiga M, Sasamoto K, Ohkura Y, Ueno K. A combined assay of cell viability and in vitro cyto-toxicity with a highly water-soluble tetrazolium salt, neutral red and crystal violet. Biol Pharm Bull. 1996;19:1518–1520.

15 Miller T, Beausang LA, Meneghini M, Lidgard G. Death-induced changes to the nuclear matrix: the use of anti-nuclear

matrix antibodies to study agents of apoptosis. Biotechniques. 1993;15:1042–1047.

16 Tang H, Guo DF, Porter JP, Wanaka Y, Inagami T. Role of cytoplasmic tail of the type 1A angiotensin II receptor in agonist- and phorbol ester-induced desensitization. Circ Res. 1998;82:523–531.

17 Al-Rawithi S, Hussein RF, Alzahrani A. Sensitive assay for the determination of fluvastatin in plasma utilizing high-performance liquid chromatography with fluorescence detection. Ther Drug Monit. 2003;25:88–92.

18 Kaneta S, Satoh K, Kano S, Kanda M, Ichihara K. All hydro-phobic HMG-CoA reductase inhibitors induce apoptotic death in rat pulmonary vein endothelial cells. Atherosclerosis. 2003;170:237–243.

19 Koga T, Shimada Y, Kuroda M, Tsujita Y, Hasegawa K, Yamazaki M. Tissue-selective inhibition of cholesterol synthesis in vivo by pravastatin sodium, a 3-hydroxy-3-methylglutaryl coenzyme A reductase inhibitor. Biochim Biophys Acta. 1990;1045:115–120.

20 Ichihara K, Satoh K. Disparity between angiographic regression and clinical event rates with hydrophobic statins. Lancet. 2002;359:2195–2198.

21 Yamazaki M, Suzuki H, Hanano M, Tokui T, Kamai T, Sugiyama Y. Sodium-independent multispecific anion trans-porter mediates active transport of pravastatin into rat liver. Am J Physiol. 1993;264:36–44.

22 Sakamoto K, Honda T, Yokoya S, Waguri S, Kimura J. Rab-small GTPases are involved in fluvastatin and pravastatin-induced vacuolation in rat skeletal myofibers. FASEB J. 2007;21:4087–4094.

23 Vu D, Murty M, McMorran M. Statins: rhabdomyolysis and myopathy. CMAJ. 2002;166:85–86.